Journal of Molecular Spectroscopy 255 (2009) 63–67

Contents lists available at ScienceDirect

Journal of Molecular Spectroscopy

journal homepage: www.elsevier.com/locate/jms

High-resolution laser spectroscopy of BaOH and BaOD: Anomalous spin-orbit coupling in the $\tilde{A}^2\Pi$ state

J.D. Tandy, J.-G. Wang, P.F. Bernath *

Department of Chemistry, University of York, Heslington, York YO10 5DD, UK

ARTICLE INFO

Article history:
Received 24 February 2009
Available online 17 March 2009

Keywords:
High-resolution
Laser excitation
BaOH
BaOD

ABSTRACT

The $\tilde{A}^2\Pi(000) - \tilde{X}^2\Sigma^+(000)$ transition of BaOD has been rotationally analyzed using laser excitation spectroscopy. BaOD molecules were synthesized through the reaction of Ba atoms with D_2O in a Broida-type oven. Rotational and fine structure parameters determined for the $\tilde{A}^2\Pi(000)$ state of BaOD yielded a spin-orbit coupling constant A significantly different from the corresponding value for BaOH ($\sim$605.8 cm^{-1} versus 560.1 cm^{-1}). Λ-doubling constants for the $\tilde{A}^2\Pi$ state were observed to be in poor agreement with the predictions of the pure precession model for the interaction between the $\tilde{A}^2\Pi$ and the $\tilde{B}^2\Sigma^+$ states in BaOD. Explanations for the unusual spin-orbit splitting and apparent failure of the pure precession and unique perturber models in BaOH and BaOD are discussed, with particular reference to possible global and local perturbations arising from vibrationally excited bands of the $\tilde{A}'^2\Delta$ state.

1. Introduction

The perturbations between the low-lying $\tilde{B}^2\Sigma^+$ and $\tilde{A}^2\Pi$ electronic states in most of the alkaline earth monohalides and monohydroxides have been observed to obey the "pure precession" model [1–5] and are believed to form a "unique perturber pair" [6] with:

$$p(\tilde{A}^2\Pi) = \frac{2A_{SO}Bl(l+1)}{E(\tilde{A}^2\Pi) - E(\tilde{B}^2\Sigma^+)}, \quad (1)$$

$$q = \frac{2B^2l(l+1)}{E(\tilde{A}^2\Pi) - E(\tilde{B}^2\Sigma^+)}, \quad (2)$$

and

$$p(\tilde{A}^2\Pi) \approx \gamma(\tilde{B}^2\Sigma^+), \quad (3)$$

where B is the rotational constant, A_{SO} is the spin-orbit constant of the $^2\Pi$ state, l is the effective quantum number of atomic orbital angular momentum, E is the energy, γ is the spin-rotation constant of the Σ state and p and q are the Λ-doubling constants of the Π state. For example, Berg et al. reported a generally good agreement between the experimental and calculated values of γ, p and q in the $B^2\Sigma^+$ and $A^2\Pi$ electronic states of CaF and showed that $p(A^2\Pi) \approx \gamma(B^2\Sigma^+)$ in this case [1]. Similarly, Steimle et al. found the $B^2\Sigma^+$ and $A^2\Pi$ states were well described by the pure precession model and observed essentially identical p and γ values [2]. The $\tilde{A}^2\Pi$ excited state of CaOH was investigated by Hilborn et al. who again found a good agreement between the p value calculated via the pure precession model and measured spectroscopically [3]. Bernath and Kinsey-Nielsen then reported good agreement between this p value and γ in the $\tilde{B}^2\Sigma^+$ state of CaOH [7]. Similar results have also been observed for the $\tilde{B}^2\Sigma^+$ and $\tilde{A}^2\Pi$ states of SrOH [4,8].

We recently reported the first high resolution analysis of the $\tilde{A}^2\Pi - \tilde{X}^2\Sigma^+$ transition of BaOH [9]. It was demonstrated that the pure precession model and unique perturber approximation are not valid for the $\tilde{B}^2\Sigma^+$ and $\tilde{A}^2\Pi$ states. It was proposed that perturbations from the closely lying $\tilde{A}'^2\Delta$ state were the source of the problems. Further investigation is therefore required to ascertain the degree of mutual global and local perturbations among the $\tilde{B}^2\Sigma^+$, $\tilde{A}^2\Pi$ and $\tilde{A}'^2\Delta$ states of BaOH.

The perturbations of BaOD should be somewhat different from those of BaOH, due to the difference in vibrational and rotational levels. Therefore the $\tilde{A}^2\Pi(000) - \tilde{X}^2\Sigma^+(000)$ transition of BaOD is expected to provide useful complementary information on the perturbations in the low-lying electronic states. This paper reports the results from our high-resolution study of the $\tilde{A}^2\Pi(000)-\tilde{X}^2\Sigma^+(000)$ transition of BaOD using laser excitation spectroscopy. Rotational and fine structure constants have been determined for the $\tilde{A}^2\Pi(000)$ state through a combined least-squares fit. A surprisingly different spin-orbit constant for the $\tilde{A}^2\Pi$ state of BaOD from that of BaOH was observed; potential explanations are discussed based on the possible perturbations occurring between the $\tilde{B}^2\Sigma^+$, $\tilde{A}^2\Pi$ and $\tilde{A}'^2\Delta$ states.

* Corresponding author. Fax: +44 1904 432516.
E-mail address: pfb500@york.ac.uk (P.F. Bernath).

0022-2852/$ - see front matter © 2009 Elsevier Inc. All rights reserved.
doi:10.1016/j.jms.2009.03.002

2. Experimental

BaOD molecules were synthesised via the reaction of D_2O vapour with Ba atoms in a Broida-type oven as previously described by Yu et al. in their analysis of SrOD [10]. The $\tilde{A}^2\Pi - \tilde{X}^2\Sigma^+$ transitions of both BaOH and BaOD were recorded via laser excitation spectroscopy. The output from a cw single-mode titanium:sapphire laser (Coherent 899-29) was focused vertically into the reaction chamber of the Broida oven with a typical laser power of ~450 mW. As the laser was scanned, the excitation fluorescence from the $\tilde{A}^2\Pi$ state was collected using a photomultiplier tube (PMT).

To improve the signal-to-noise ratio of the fluorescence signal, a 0.32 m monochromator was employed as either a spatial filter for total fluorescence scans, (monochromator set to zero-order) or as a band-pass filter for recording excitation spectra. With the monochromator set at zero-order it was possible to locate a number of vibrational bands by scanning the laser over a large spectral range. The laser was then fixed at the band head of interest while the monochromator was tuned until the strongest fluorescence signal was obtained. This monochromator position was then maintained whilst the laser was scanned through the required spectral range to obtain the high-resolution spectrum. The majority of bands obtained using this method were clear and easily assigned.

Phase sensitive detection was employed using a mechanical chopper to modulate the titanium:sapphire laser beam and a lock-in amplifier was used to process the fluorescence signal from the PMT. Spectra were recorded in 5 cm^{-1} segments at a scan speed of 2 GHz per second with a data sampling interval of 50 MHz. The absolute frequency of the laser was calibrated by simultaneously recording the absorption spectrum of a heated I_2 cell [11].

3. Results and analysis

In the previous low-resolution work, band heads at ~11 467 and 12 039 cm^{-1} were assigned to the $\tilde{A}^2\Pi_{1/2}(000) - \tilde{X}^2\Sigma^+(000)$ and $\tilde{A}^2\Pi_{3/2}(000) - \tilde{X}^2\Sigma^+(000)$ transitions of BaOD, respectively [12]. The recent high resolution analysis of the $\tilde{A}^2\Pi - \tilde{X}^2\Sigma^+$ transition of BaOH [9] yielded band heads for the $\tilde{A}^2\Pi_{1/2}(000) - \tilde{X}^2\Sigma^+(000)$ and $\tilde{A}^2\Pi_{3/2}(000) - \tilde{X}^2\Sigma^+(000)$ transitions at 11 484.286 and 12 046.933 cm^{-1}, respectively. High-resolution scans were performed based on these assignments to accurately locate the position of the two corresponding band heads for BaOD.

Fig. 1 shows an overview of the high-resolution spectra of the $\tilde{A}^2\Pi_{1/2}(000) - \tilde{X}^2\Sigma^+(000)$ (upper panel) and $\tilde{A}^2\Pi_{3/2}(000) - \tilde{X}^2\Sigma^+(000)$ (lower panel) transitions, plotted on a relative wavenumber scale in a spectral range of ~100 cm^{-1}. As illustrated, $\tilde{A}^2\Pi(000) - \tilde{X}^2\Sigma^+(000)$ transition bands for both BaOH and BaOD were observed in the spectra. The presence of BaOH molecules can be explained by residual sources of water vapour in the Broida oven, originating from both the Ar and D_2O gas inlets.

Table 1 summarises the band head positions of the observed transitions in this investigation and shows that in addition to the $\tilde{A}^2\Pi(000) - \tilde{X}^2\Sigma^+(000)$ bands of BaOH and BaOD, four unassigned bands (B1–B4) were observed in the spectral range of the $\tilde{A}^2\Pi(001) - \tilde{X}^2\Sigma^+(000)$ transitions of BaOH and BaOD. The spectra of the two sub-bands in each of the $\tilde{A}^2\Pi(000)$- $\tilde{X}^2\Sigma^+(000)$ transitions exhibit a Hund's case (a) $^2\Pi$ – Hund's case (b) $^2\Sigma^+$ pattern with a clear $1B$ Q_{fe}/R_{ff} band head and the R_{ff}/Q_{fe} and P_{ee}/Q_{ef} paired lines [13]. Unfortunately, bands B1–B4 were not rotationally assignable due to calibration difficulties caused by problems in scanning the laser in these regions and therefore could be from either BaOH or BaOD. Fig. 1 also highlights some weaker head-like features observed in the spectra (labelled by asterisks), likely originating from excited vibrational states of the $\tilde{A}'^2\Delta - \tilde{X}^2\Sigma^+$ transition [12] of either BaOH or BaOD. The intensity distribution of the observed lines in each spectrum is affected by the position and bandwidth of the monochromator, as well as changes in the oven conditions during the laser scan.

Fig. 2 shows the band heads for the $\tilde{A}^2\Pi_{3/2}(000) - \tilde{X}^2\Sigma^+(000)$ (upper panel) and $\tilde{A}^2\Pi_{1/2}(000)$- $\tilde{X}^2\Sigma^+(000)$ (lower panel) transitions of BaOD with their rotational (J) assignments presented

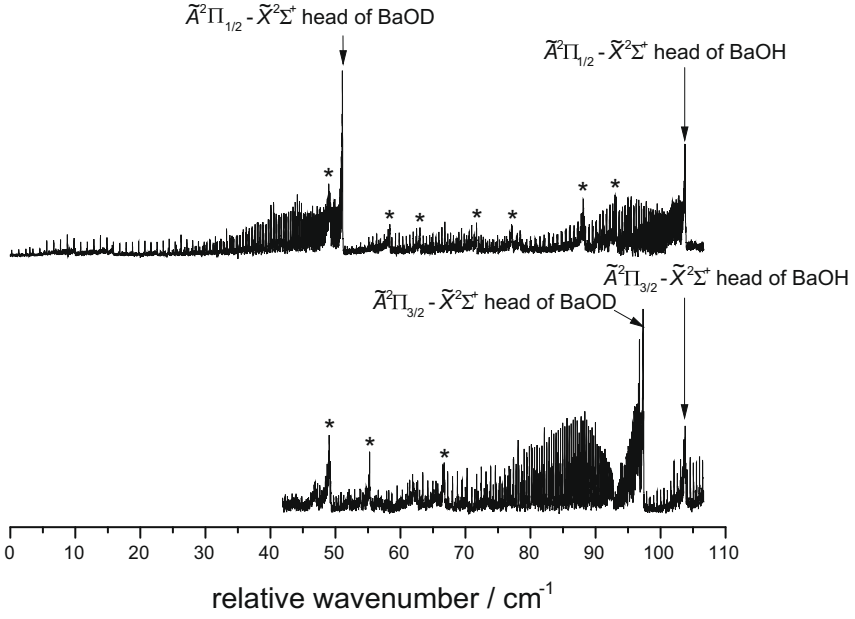

Fig. 1. The high-resolution laser excitation spectra of the $\tilde{A}^2\Pi_{1/2}(000) - \tilde{X}^2\Sigma^+(000)$ (upper panel) and $\tilde{A}^2\Pi_{3/2}(000) - \tilde{X}^2\Sigma^+(000)$ (lower panel) transitions of BaOH and BaOD on a relative wavenumber scale in the spectral range of ~100 cm^{-1}. The wavenumber zero for the $\tilde{A}^2\Pi_{1/2}(000) - \tilde{X}^2\Sigma^+(000)$ scan is 11 380.506 cm^{-1} while the $\tilde{A}^2\Pi_{3/2}(000) - \tilde{X}^2\Sigma^+(000)$ scan starts at 11 985.021 cm^{-1}. The spectra were recorded by scanning a single-mode ring titanium:sapphire laser and monitoring the fluorescence through a 0.32 m monochromator. The two spectra are aligned on the respective BaOH band heads of each transition. All 6 branches of the BaOD transitions were observed and assigned for each transition. Other head-like features (marked by asterisks) are likely to arise from excited vibrational bands of the $\tilde{A}'^2\Delta - \tilde{X}^2\Sigma^+$ transition.

Table 1
Observed band heads (in cm^{-1}).

Molecule	Band head	Transition or band
BaOH	11 484.286	$\tilde{A}^2\Pi_{1/2}(000) - \tilde{X}^2\Sigma^+(000)$
	12 046.933	$\tilde{A}^2\Pi_{3/2}(000) - \tilde{X}^2\Sigma^+(000)$
BaOD	11 431.577	$\tilde{A}^2\Pi_{1/2}(000) - \tilde{X}^2\Sigma^+(000)$
	12 040.464	$\tilde{A}^2\Pi_{3/2}(000) - \tilde{X}^2\Sigma^+(000)$
Unassigned	11 896.331	B1
	12 505.159	B2
	11 877.839	B3
	12 490.569	B4

above. As the figure illustrates, the shape of the two band heads are clearly different with the R_{22} turning point approximately 0.1 cm^{-1} from the Q_{21} turning position, producing a clear R_{22} sub-head of the $\tilde{A}^2\Pi_{3/2}(000) - \tilde{X}^2\Sigma^+(000)$ transition. However, for the $\tilde{A}^2\Pi_{1/2}(000) - \tilde{X}^2\Sigma^+(000)$ transition spectrum, a small shoulder is formed by the R_{12} branch turning point due to the relatively low J'' value.

The rotational assignments for the observed bands of BaOD were made using lower state combination differences in the $\tilde{X}^2\Sigma^+$ state [14]. About 839 lines in 12 branches of the $\tilde{A}^2\Pi(000) - \tilde{X}^2\Sigma^+(000)$ transition were assigned and the measured lines modelled using standard Hund's case (a) $^2\Pi$ – Hund's case (b) $^2\Sigma^+$ Hamiltonians [15]. A combined least-squares fit was performed, which included the 839 lines of the $\tilde{A}^2\Pi(000) - \tilde{X}^2\Sigma^+(000)$ transition (this work) and 24 pure rotational lines of the $\tilde{X}^2\Sigma^+(000)$ state [14]. Each line in the fit was weighted according to its experimental uncertainty. For the millimeter-wave data [14] an estimated uncertainty of 10^{-6} cm^{-1} was used, while for the optical data of this work an uncertainty of 0.005 cm^{-1} was applied. The effective higher order constants A_H and p_D were required to obtain a good fit of the measured spectral lines for the $\tilde{A}^2\Pi(000) - \tilde{X}^2\Sigma^+(000)$ transition. The spectroscopic constants generated from the combined least-squares fit for the $\tilde{X}^2\Sigma^+(000)$ and $\tilde{A}^2\Pi(000)$ electronic states of BaOD are given in Table 2.

To further confirm the identification of the sub-states $\tilde{A}^2\Pi_{3/2}(000)$ and $\tilde{A}^2\Pi_{1/2}(000)$, least-squares fits of the bands using the Hund's case (c) expression:

$$F(J) = BJ(J+1) - D[J(J+1)]^2 + H[J(J+1)]^3 + L[J(J+1)]^4 \pm 1/2(J+1/2)[p + p_D(J+1/2)^2 + p_H(J+1/2)^4 + p_L(J+1/2)^6], \quad (4)$$

(where B, D, H and L are rotational constants and p, p_D, p_H and p_L are Ω-doubling constants), were performed for the excited states. The ± sign in Eq. (4) refers to the e- (+) and f-parity (−) levels, respectively. The analysis was carried out using the same method utilised when fitting the three unidentified bands (U1–U3) in our previous analysis of the $\tilde{A}^2\Pi - \tilde{X}^2\Sigma^+$ transition of BaOH [9]. Table 3 illustrates the spectroscopic constants generated from the Hund's case (c) combined fits for the $\tilde{A}^2\Pi_{3/2}(000)$, $\tilde{A}^2\Pi_{1/2}(000)$ and $\tilde{X}^2\Sigma^+(000)$ states of BaOD. In addition, the (previously unreported) corresponding Hund's case (c) spectroscopic constants for the $\tilde{A}^2\Pi_{3/2}(000)$, $\tilde{A}^2\Pi_{1/2}(000)$ and $\tilde{X}^2\Sigma^+(000)$ electronic states of BaOH are also presented for comparison. The measured lines for all observed bands in the $\tilde{A}^2\Pi(000) - \tilde{X}^2\Sigma^+(000)$ transitions of BaOD are provided as supplementary material from this journal.

4. Discussion

The assignment of the various band heads observed in this work to specific electronic transitions requires some consideration. The two band head positions previously assigned to the $\tilde{A}^2\Pi(000)-\tilde{X}^2\Sigma^+(000)$ transitions of BaOH [9] are a useful starting point in the search for the corresponding $\tilde{A}^2\Pi(000) - \tilde{X}^2\Sigma^+(000)$ bands of BaOD. The isotope shift caused by deuteration of BaOH was expected to be relatively small (e.g. ~6 cm^{-1} for SrOH/SrOD [8,10]). Interestingly, as can be seen in Fig. 1, the two band heads assigned to the $\tilde{A}^2\Pi(000) - \tilde{X}^2\Sigma^+(000)$ transition of BaOD are separated from their corresponding BaOH band heads by considerably differing amounts.

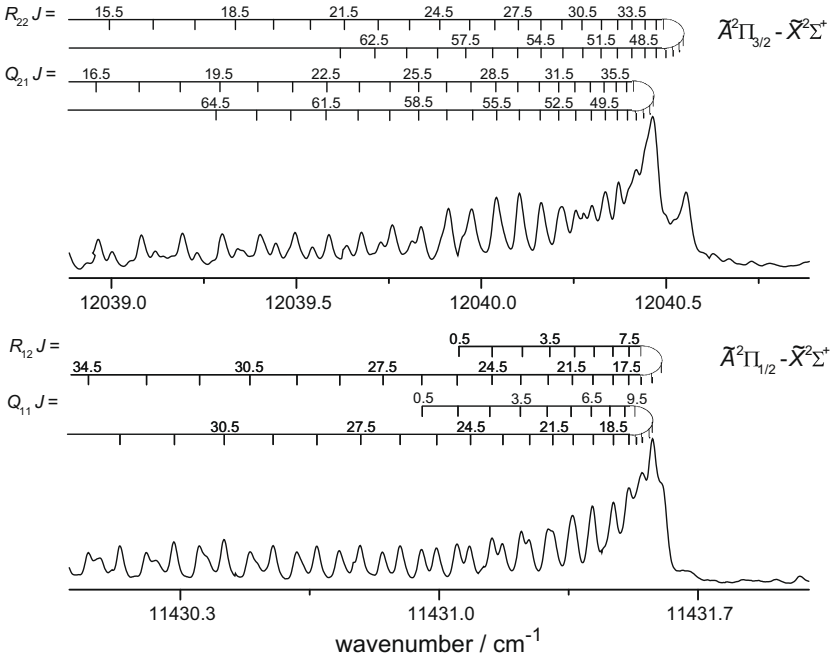

Fig. 2. An expanded portion of the laser excitation spectrum corresponding to the R/Q branch heads of the $\tilde{A}^2\Pi_{3/2}(000) - \tilde{X}^2\Sigma^+(000)$ (upper panel) and $\tilde{A}^2\Pi_{1/2}(000) - \tilde{X}^2\Sigma^+(000)$ (lower panel) transitions of BaOD. J'' assignments of the R_{22}, Q_{21}, R_{12} and Q_{11} branches are presented above the spectrum. The R_{12} branch forms a branch head at $J'' \sim 15.5$ in the $\tilde{A}^2\Pi_{1/2}(000)$- $\tilde{X}^2\Sigma^+(000)$ transition, as compared to the R_{22} branch of the $\tilde{A}^2\Pi_{3/2}(000)$- $\tilde{X}^2\Sigma^+(000)$ transition that forms a branch head at $J'' \sim 41.5$. This results in the appearance of a large shoulder ~0.1 cm^{-1} from the Q_{21} branch head of the $\tilde{A}^2\Pi_{3/2}(000)$- $\tilde{X}^2\Sigma^+(000)$ transition.

Table 2
Spectroscopic constants (in cm^{-1}) for BaOD[a].

Constant	$\tilde{X}^2\Sigma(000)$[b]	$\tilde{A}^2\Pi(000)$[b]
T	0.0	11 733.58419(19)
B	0.195751870(93)	0.19271712(24)
$D \times 10^{-7}$	1.26316(63)	1.2268(79)
$\gamma \times 10^{-3}$	2.1734(21)	
A		605.83684(37)
$A_D \times 10^{-3}$		1.42803(46)
$A_H \times 10^{-8}$		−0.6909(47)
$q \times 10^{-5}$		1.44(42)
p		−0.179378(17)
$p_D \times 10^{-6}$		−2.2757(48)

[a] Values in parentheses are 1σ standard deviations, in units of the last significant digits.
[b] Constants were generated by a combined fit of the $\tilde{A}^2\Pi - \tilde{X}^2\Sigma^+$ transition data and the millimeter-wave data of the $\tilde{X}^2\Sigma^+$ state [14] and a Hund's case (a) $^2\Pi$ Hamiltonian.

The observed isotope shift for the $\tilde{A}^2\Pi_{1/2}(000) - \tilde{X}^2\Sigma^+(000)$ spin component is approx. $-52.7\ cm^{-1}$ in comparison to approx. $-6.5\ cm^{-1}$ (Table 1) for the $\tilde{A}^2\Pi_{3/2}(000) - \tilde{X}^2\Sigma^+(000)$ transition.

Fig. 1 clearly demonstrates that the band at 11 431.577 cm^{-1} (relative frequency ~50 cm^{-1}) was the only prominent band head observed in this region of the spectrum and is therefore the most likely to correspond to the $\tilde{A}^2\Pi_{1/2}(000) - \tilde{X}^2\Sigma^+(000)$ transition of BaOD. The band head at 12 040.464 cm^{-1} for the $\tilde{A}^2\Pi_{3/2}(000) - \tilde{X}^2\Sigma^+(000)$ transition seems reasonable based upon a similar observation in the previous low-resolution work at ~12 039 cm^{-1} [12]. However the band head for the $\tilde{A}^2\Pi_{1/2}(000) - \tilde{X}^2\Sigma^+(000)$ transition of BaOD differs considerably (11 431.577 cm^{-1} compared to 11 467 cm^{-1}). Presumably there was an error in the calibration of the laser in the previous low-resolution analyses.

To further justify this assignment an investigation was carried out to observe the $\tilde{A}^2\Pi(000) - \tilde{X}^2\Sigma^+(000)$ band heads of BaOH and BaOD whilst varying the reactant vapour between D_2O and H_2O_2. The experiment showed a considerable decrease in the intensity of the two BaOD $\tilde{A}^2\Pi(000) - \tilde{X}^2\Sigma^+(000)$ band heads (until they were no longer observed), in addition to a significant increase in the two $\tilde{A}^2\Pi(000) - \tilde{X}^2\Sigma^+(000)$ band heads of BaOH when the reactant was switched to H_2O_2. Similarly, when the reactant was changed back to D_2O, the intensity of the BaOH band heads decreased and those of BaOD returned to their original intensity. These observations unambiguously confirmed the assignment of the band heads at 11 431.577 cm^{-1} and 12 040.464 cm^{-1} to transitions of BaOD.

It is also interesting to compare the molecular constants generated in the least-squares fit using both the Hund's case (a) and Hund's case (c) expressions for the upper states in BaOH (Ref. [9]) and BaOD (this work). Table 3 reveals that when using the Hund's case (c) expressions in the fit, the B values yielded for the $\tilde{A}^2\Pi_{1/2}$ and $\tilde{A}^2\Pi_{3/2}$ states differ slightly for both BaOH and BaOD, (~0.2111 versus 0.2136 cm^{-1} and ~0.1919 versus 0.1935 cm^{-1} respectively). Furthermore, it was shown that the Ω-doubling parameters p and p_D were well defined in the Hund's case (c) fits for the bands assigned to the $\tilde{A}^2\Pi_{1/2}(000) - \tilde{X}^2\Sigma^+(000)$ transitions in both BaOH and BaOD, but were not present in either of the fits for the bands assigned to the $\tilde{A}^2\Pi_{3/2}(000) - \tilde{X}^2\Sigma^+(000)$ transitions. This similarity between the $\tilde{A}^2\Pi_{1/2}$ case (c) fit constants for BaOH and BaOD further supports the assignment of the 11 431 cm^{-1} band to the $\tilde{A}^2\Pi_{1/2}(000) - \tilde{X}^2\Sigma^+(000)$ transition of BaOD.

Given these assignments it is appropriate to consider why the $\tilde{A}^2\Pi$ states of BaOH and BaOD exhibit such a large difference in their spin-orbit splitting (~45 cm^{-1}). Theoretically the spin-orbit constant, A should be identical in both isotopologues. Indeed, the difference in the observed spin-orbit splittings of the $\tilde{A}^2\Pi$ state in SrOH [8] and SrOD [10] is only ~1 cm^{-1}. As Table 2 illustrates, this is clearly not the case in BaOH and BaOD. It is therefore reasonable to conclude, based on this observation, that the $\tilde{A}^2\Pi$ states of BaOH and/or BaOD are globally perturbed as previously proposed [9].

Further examination of the Λ-doubling constants generated in the Hund's case (a) fit reveal a p value of $-0.179378\ cm^{-1}$ and a q value of $1.44 \times 10^{-5}\ cm^{-1}$ in the $\tilde{A}^2\Pi$ state of BaOD (Table 2). Using the pure precession model, Eq. (1) with an effective $l = 1$, $E(\tilde{B}^2\Sigma^+) = 13\,173.469\ cm^{-1}$ [16] and the $E(\tilde{A}^2\Pi)$, $A_{SO}(\tilde{A}^2\Pi)$ and B values determined in this work (Table 2) we can calculate $p(\tilde{A}^2\Pi) = -0.3243\ cm^{-1}$. This value differs considerably from both the spin-rotation constant of the $\tilde{B}^2\Sigma^+$ state (approx. $-0.2285\ cm^{-1}$) [16] and our observed value for $p(\tilde{A}^2\Pi)$. Furthermore, the observed q value in this investigation is positive, which should clearly not be the case according to Eq. (2). These trends mimic almost exactly those observed in our previous analysis of the $\tilde{A}^2\Pi$ state of BaOH [9]. It therefore reasonable to conclude that the pure precession model is not at all appropriate for the $\tilde{B}^2\Sigma^+$ and $\tilde{A}^2\Pi$ states of both BaOH and BaOD and that the unique perturber approximation is also not valid.

The apparent failure in the unique perturber approximation suggests that the $\tilde{A}^2\Pi$ state of BaOH may have a significant interaction with a closely lying electronic state other than the $\tilde{B}^2\Sigma^+$ state. The previously observed $\tilde{A}'^2\Delta$ state of BaOH [12] could be expected to interact relatively strongly with the closely lying $\tilde{A}^2\Pi$ state. The $\tilde{A}^2\Pi_{1/2}(000)$ spin component is particularly affected, so it is possible that a $^2\Pi_{1/2}$ vibronic state from the $\tilde{A}'^2\Delta$ state [17], may happen to lie very close in energy to the $\tilde{A}^2\Pi_{1/2}$ state of BaOH. Mixing of these two $^2\Pi_{1/2}$ states could therefore cause significant local perturbations and potentially disrupt the unique perturber pair approximation of the $\tilde{B}^2\Sigma^+$ and $\tilde{A}^2\Pi$ states.

Λ-doubling is known to be very small in Δ electronic states [18]. It may therefore be expected that mixing of the $\tilde{A}^2\Pi$ state with a vibronic level of a closely lying Δ state would reduce Λ-doubling and consequently yield a smaller observed p value than

Table 3
Spectroscopic constants (in cm^{-1}) for BaOH and BaOD.[a]

Constant	BaOH		BaOD	
	$\tilde{A}^2\Pi_{1/2}(000)$[b]	$\tilde{A}^2\Pi_{3/2}(000)$[b]	$\tilde{A}^2\Pi_{1/2}(000)$[b]	$\tilde{A}^2\Pi_{3/2}(000)$[b]
T	11 483.44476(55)	12 043.13030(40)	11 430.90580(23)	12 036.35757(29)
B	0.211068153(79)	0.213636661(51)	0.191941564(25)	0.19349211(36)
$D \times 10^{-7}$	1.4844(26)	1.7487(15)	1.15512(72)	1.29808(81)
$H \times 10^{-13}$	−1.83(23)			
p	0.146118(24)		0.179354(14)	
$p_D \times 10^{-6}$	2.5070(50)		2.2650(36)	

[a] Values in parentheses are 1σ standard deviation, in units of the last significant digits.
[b] Constants generated by a combined fit of the $\tilde{A}^2\Pi - \tilde{X}^2\Sigma^+$ transition data and the millimeter-wave data of the $\tilde{X}^2\Sigma^+$ state [14,19] and a Hund's case (c) expression for the $\tilde{A}^2\Pi$ two spin components.

Table 4
Bond lengths (Å) of BaOH.

	$\tilde{X}^2\Sigma^+$[a]	$\tilde{A}^2\Pi$[b]	$\tilde{B}^2\Sigma^+$[c]
r_0 (BaO)	2.200	2.237	2.231
r_0 (OH)	0.927	0.758*	0.909

[a] Determined from millimeter-wave data of BaOH and BaOD [14].
[b] Determined from optical data of BaOH and BaOD (this work).
[c] Determined from optical data of BaOH and BaOD [16].
* The derived OH bond length is too short for a linear molecule, as discussed in the text.

the calculated p value from the pure precession model. This could at least partially explain the apparent failure of the pure precession model to describe the interactions of the $\tilde{B}^2\Sigma^+$ and $\tilde{A}^2\Pi$ states of BaOH. Furthermore, global perturbations would be expected to shift the observed origin of the $\tilde{A}^2\Pi_{1/2}(000) - \tilde{X}^2\Sigma^+(000)$ transition, explaining the discrepancy in the spin-orbit coupling parameters for BaOH and BaOD.

Another indication of the effects of these perturbations is demonstrated in the calculation of the bond lengths, r_0 for the $\tilde{A}^2\Pi$ state of BaOH. Bond lengths were also calculated for the $\tilde{B}^2\Sigma^+$ state of BaOH, using an average of the e and f-parity B values derived by Kinsey-Nielsen et al. in their spectroscopic analysis of BaOH and BaOD [16]. Table 4 lists the bond lengths for the $\tilde{B}^2\Sigma^+$, $\tilde{A}^2\Pi$ and $\tilde{X}^2\Sigma^+$ states of BaOH. There is a clear discrepancy between the OH bond length of the $\tilde{A}^2\Pi$ state calculated using the rotational constants in this work and those of the $\tilde{B}^2\Sigma^+$ and $\tilde{X}^2\Sigma^+$ states. An OH bond length of 0.758 Å is unrealistically small for a linear molecule, particularly when compared to the $\tilde{B}^2\Sigma^+$ and $\tilde{X}^2\Sigma^+$ state values (~0.9 Å). The BaO bond length of the $\tilde{A}^2\Pi$ state however, is reasonably close to that of the $\tilde{B}^2\Sigma^+$ state and shows no clear sign of discrepancy.

A similar observation was noted by Yu et al. when studying the $\tilde{C}^2\Pi$ state of SrOH [10]. They suggested that global perturbations of this state may have given different non-mechanical contributions to their derived B values resulting in anomalous bond lengths. It therefore seems reasonable to conclude that the potentially large perturbations in BaOH and BaOD is likely responsible for the apparently anomalous bond lengths observed in the $\tilde{A}^2\Pi$ state. The other major factor that could explain the significantly smaller OH bond length is the possibility of large amplitude bending in the $\tilde{A}^2\Pi$ transitions for both BaOH and BaOD. This would cause the calculated bond length to correspond to an average of the projections on the molecular axis, leading to an underestimation of the true OH bond length. Such a large amplitude bending motion however, would imply a low bending frequency and a long progression in the bending mode that is not observed.

Although the identification of the $\tilde{A}^2\Pi_{1/2}$ spin components for BaOH and BaOD is supported by the evidence mentioned above, it is possible that the observed bands may originate from excited vibrational bands of the $\tilde{A}^2\Pi - \tilde{X}^2\Sigma^+$ or $\tilde{A}'^2\Delta - \tilde{X}^2\Sigma^+$ transition of BaOH and BaOD. These potential misidentifications could also explain the apparent discrepancy between the A values of BaOH and BaOD, as excited vibrational bands of the two isotopologues would be clearly separated due to their different vibrational frequencies. These uncertainties mean that the assignments given for the $\tilde{A}^2\Pi - \tilde{X}^2\Sigma^+$ transitions of BaOH and BaOD (particularly for the $^2\Pi_{1/2}$ spin component) should be, at the current time, viewed with a degree of caution.

A detailed examination of the $\tilde{A}'^2\Delta$ state is now required to further understand the nature of the interactions between the $\tilde{B}^2\Sigma^+$, $\tilde{A}^2\Pi$ and $\tilde{A}'^2\Delta$ states of BaOH. To this end, a V-type optical–optical double resonance spectroscopy experiment is underway to locate the lower-lying excited state levels of BaOH. These bands are inaccessible by direct fluorescence detection with our current photomultiplier tube because of the low sensitivity in this spectral region. Preliminary results indicate that there is indeed a band in close proximity just on the lower wavenumber side of the $\tilde{A}^2\Pi_{1/2}$ sub-state of BaOH (at ~11 306 cm^{-1}). Furthermore, initial analysis yielded a relatively large p value, suggesting some $\Pi_{1/2}$ character in the excited state of this band, but work is still in progress.

5. Conclusions

The $\tilde{A}^2\Pi(000) - \tilde{X}^2\Sigma^+(000)$ transition of BaOD has been rotationally analyzed using laser excitation spectroscopy. The measured rotational lines of BaOD were fitted in combination with the millimeter-wave pure rotational data of the $\tilde{X}^2\Sigma^+$ state [14]. Rotational and fine structure constants have been determined for the $\tilde{A}^2\Pi(000)$ state using the standard Hund's case (a) $^2\Pi$ Hamiltonian [15]. The corresponding constants were also derived for the $\tilde{A}^2\Pi_{3/2}(000)$ and $\tilde{A}^2\Pi_{1/2}(000)$ spin components of BaOH and BaOD individually, by fitting the excited states using a Hund's case (c) energy level expression. These analyses yield a considerable difference in the spin-orbit constant A, for BaOH and BaOD and this difference is believed to result from strong global perturbations originating from the lower-lying $\tilde{A}'^2\Delta$ state. Strong perturbations are also indicated by the apparent failure of the pure precession and unique perturber models in both BaOH and BaOD and the unrealistic OH bond length calculated from the B values of the $\tilde{A}^2\Pi$ states. In order to further understand the nature of the interactions between the $\tilde{B}^2\Sigma^+$, $\tilde{A}^2\Pi$ and $\tilde{A}'^2\Delta$ states of BaOH a detailed analysis of the $\tilde{A}'^2\Delta$ state is now required; these experiments are currently in progress.

Acknowledgment

This research was supported by funding from EPSRC.

Appendix A. Supplementary data

Supplementary data for this article are available on ScienceDirect (www.sciencedirect.com) and as part of the Ohio State University Molecular Spectroscopy Archives (http://library.osu.edu/sites/msa/jmsa_hp.htm).

References

[1] J.M. Berg, J.E. Murphy, N.A. Harris, R.W. Field, Phys. Rev. A: At. Mol. Opt. Phys. 48 (1993) 3012–3029.
[2] T.C. Steimle, P.J. Domaille, D.O. Harris, J. Mol. Spectrosc. 73 (1978) 441–443.
[3] R.C. Hilborn, Z. Qingshi, D.O. Harris, J. Mol. Spectrosc. 97 (1983) 73–91.
[4] J. Nakagawa, R.F. Wormsbecher, D.O. Harris, J. Mol. Spectrosc. 97 (1983) 37–64.
[5] R.S. Mulliken, A. Christy, Phys. Rev. 38 (1931) 87–119.
[6] H. Lefebvre-Brion, R.W. Field, The Spectra and Dynamics of Diatomic Molecules, Elsevier, Amsterdam, 2004.
[7] P.F. Bernath, S. Kinsey-Nielsen, Chem. Phys. Lett. 105 (1984) 663–666.
[8] C.R. Brazier, P.F. Bernath, J. Mol. Spectrosc. 114 (1985) 163–173.
[9] J.-G. Wang, J.D. Tandy, P.F. Bernath, J. Mol. Spectrosc. 252 (2008) 31–36.
[10] S. Yu, J.-G. Wang, P.M. Sheridan, M.J. Dick, P.F. Bernath, J. Mol. Spectrosc. 240 (2006) 26–31.
[11] S. Gerstenkorn, J. Verges, J. Chevillard, Atlas du Spectre d'Absorption de la Molecule d'Iode, Laboratoire Aimé Cotton, CNRS II 91405 Orsay, France, 1982.
[12] W.T.M.L. Fernando, M. Douay, P.F. Bernath, J. Mol. Spectrosc. 144 (1990) 344–351.
[13] G. Herzberg, Molecular Spectra and Molecular Structure, vol. 1, Krieger Publishing Company, Malabar, Florida, 1989.
[14] M.A. Anderson, M.D. Allen, W.L. Barclay Jr., L.M. Ziurys, Chem. Phys. Lett. 205 (1993) 415–422.
[15] J.M. Brown, E.A. Colbourn, J.K.G. Watson, F.D. Wayne, J. Mol. Spectrosc. 74 (1979) 294–318.
[16] S. Kinsey-Nielsen, C.R. Brazier, P.F. Bernath, J. Chem. Phys. 84 (1986) 698–708.
[17] P.F. Bernath, Spectra of Atoms and Molecules, second ed., Oxford University Press, USA, 2005.
[18] J.M. Brown, A.S-C. Cheung, A.J. Merer, J. Mol. Spectrosc. 124 (1987) 464–475.
[19] M.A. Anderson, W.L. Barclay Jr., L.M. Ziurys, Chem. Phys. Lett. 196 (1992) 166–172.